AMERICAN SOCIETY of
GENE & CELL
THERAPY

Long Non-coding RNA PVT1 Competitively Binds MicroRNA-424-5p to Regulate CARM1 in Radiosensitivity of Non-Small-Cell Lung Cancer

Dong Wang[1,2] and Yi Hu[1]

[1]Department of Medical Oncology, Chinese PLA General Hospital, Beijing 100853, China; [2]Department of Oncology, Affiliated Hospital of Inner Mongolia University for Nationalities, Tongliao 028000, China

Accumulating evidence revealed that dysregulated long non-coding RNAs (lncRNAs) were involved in tumorigenesis and progression. This study is supposed to reveal the effects of lncRNA PVT1 on the radiosensitivity of non-small-cell lung cancer (NSCLC) via the microRNA (miR)-424-5p/lncRNA PVT1/CARM1 signaling pathway. Differentially expressed lncRNA was filtrated. The co-expressed gene of lncRNA was predicted, and gene ontology analysis was performed to find out the genes associated with NSCLC radiosensitivity. The miR that was combined with lncRNA and mRNA was filtrated. Two cell lines with the highest expressed PVT1 were selected, followed by transfection with a series of different mimic, inhibitor, or siRNA. RIP assay was employed for the interaction between PVT1 and CARM1. The regulatory effect of miR-424-5p on cell proliferation, migration, invasion, cycle, and apoptosis was investigated. PVT1 was the most remarkable lncRNA that upregulated in NSCLC. CARM1 co-expressed with lncRNA PVT1 and associated with NSCLC radiosensitivity. Both lncRNA PVT1 and CARM1 can combine with miR-424-5p. Increased PVT1, CARM1, MMP-2, MMP-9, and Bcl-2 and decreased miR-424-5p and Bax were found in NSCLC tissues. PVT1 was targeted by miR-424-5p. After silencing of PVT1 or overexpressed miR-424-5p, decreased PVT1, CARM1, MMP-2, MMP-9, and Bcl-2 inhibited cell proliferation, migration, and invasion but promoted miR-424-5p, Bax, and cell apoptosis. The present study confirms the radiosensitivity of NSCLC radiotherapy can be increased by siRNA-PVT1 and overexpressed miR-424-5p.

INTRODUCTION

Lung cancer has long been the most concerning malignancy worldwide because it has the highest morbidity among men and the second highest among women.[1] It was also estimated that non-small-cell lung cancer (NSCLC) reached 80% of the all events of lung cancer.[2] Squamous cell carcinoma and adenocarcinoma, the primary histological types of NSCLC, present differently in respect to geography and clinic.[3] According to relative data, most patients with NSCLC are diagnosed at an advanced stage with a 5-year survival rate of <5%.[4] Smoking was identified as the major cause of this disease, which is responsible for 80% more cases.[5] Chemotherapy is the mainstay of

NSCLC treatment, but the response rate is only 30%,[6] and there are few second- or third-line treatments.[7] Therefore, it is urgent to work out a feasible method around molecule science to release the suffering of NSCLC patients.

Long non-coding RNAs (lncRNAs), a kind of RNA molecule with over 200 nucleotides, are mainly located in the cell nucleus and cytoplasm and can be further subgrouped according to their location with regard to protein-coding genes.[8] Convincing evidence suggests that lncRNAs serve as gene regulators in the microenvironment of a molecule, regulating the amount of genes and affecting various cellular pathways.[9] The plasmacytoma variant translocation 1 (PVT1), taken as an oncogene, is a sort of lncRNA located in the 8q24 gene desert, which had been found to be highly expressed in a lot of human tumors.[10] As the expression of lncRNA PVT1 in NSCLC was notably higher than that in normal lung tissues, it offered the possible role of abnormal PVT1 expression on NSCLC pathogenesis.[11] It had been verified that upregulated PVT1 led to poorer prognosis in colorectal cancer.[12] Co-activator-associated arginine methyltransferase 1 (CARM1), functioning as a co-activator, can cooperate with the protein arginine methyltransferase (PRMT) family in gene regulation and are overexpressed in the NSCLC cell line.[13] MicroRNA (miR)-424-5p is involved in the invasion and metastasis of esophageal squamous cell carcinoma.[14] A new study indicates that miR-424 was highly expressed in NSCLC tissues, especially in patients at advanced stage.[15] We find that it is now possible to work out how PVT1 affects the development of NSCLC with the cooperation of CARM1 and miR-424-5p, which is exactly the objective of our study.

RESULTS

PVT1 Was Selected for Our Study

According to the analysis of NSCLC-related microarray expression data (GEO: GSE18842 and GSE85716), PVT1 was the most strikingly
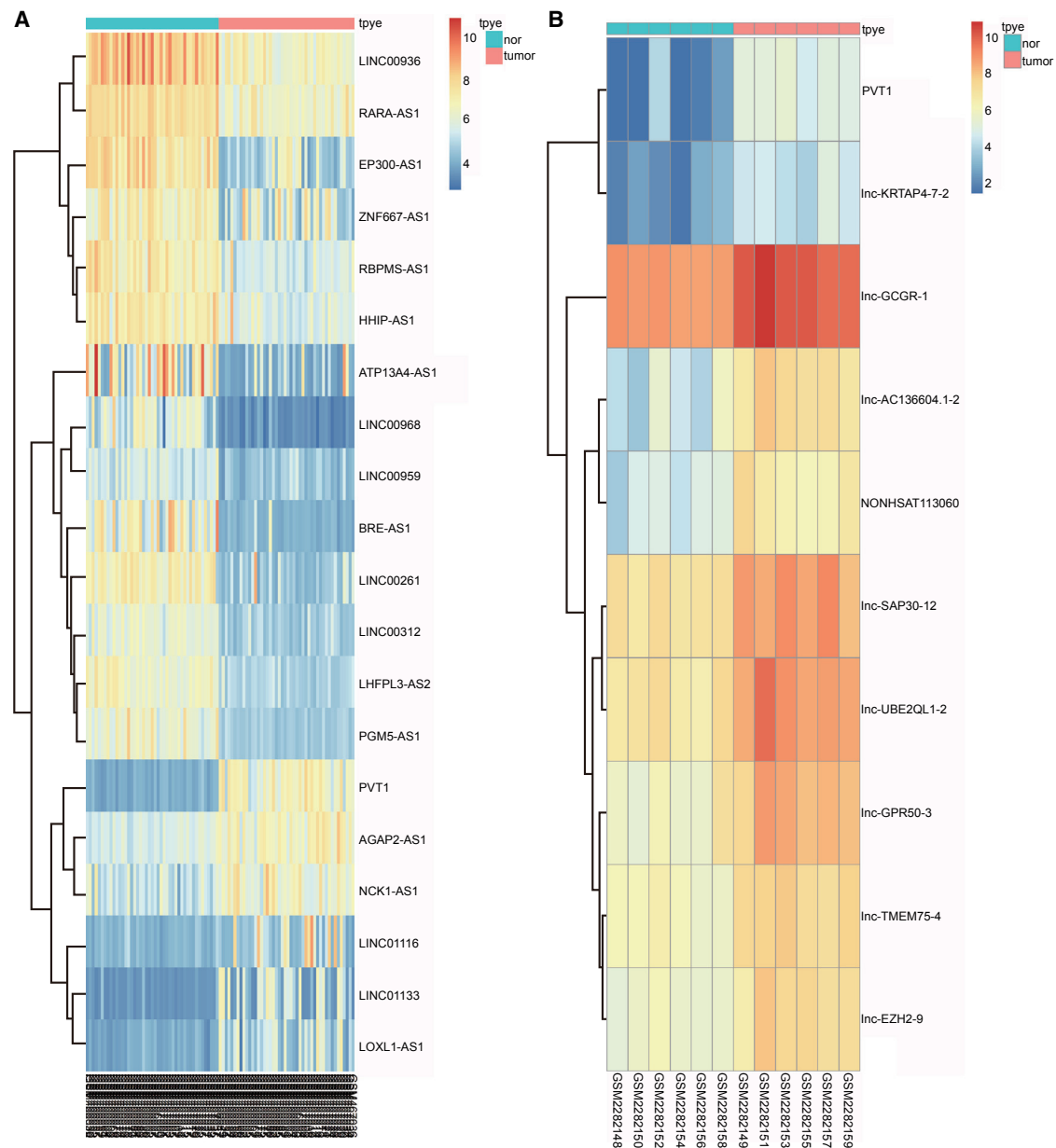
Figure 1. PVT1 Expression in NSCLC Microarray

(A) GEO: GSE18842 and (B) GEO: GSE85716. PVT1, plasmacytoma variant translocation 1; NSCLC, non-small cell lung cancer.

upregulated lncRNA in NSCLC (Figures 1A and 1B), so it was taken as the representative lncRNA in this study.

NPM1, TP53, and CARM1 Were Associated with NSCLC Radiosensitivity

The co-expressed gene of lncRNA was predicted by Multi Experiment Matrix (MEM), and gene ontology (GO) analysis was performed by the DAVID database to find the genes associated with NSCLC radiosensitivity. Among the co-expressed genes, only

NPM1, TP53, and CARM1 were associated with NSCLC radiosensitivity (Figure 2).

lncRNA PVT1 and CARM1 Can Combine with miR-424-5p

The starBase database provides the ability to filter miRNA that was combined with lncRNA, and mRNA-combing miRNA was filtered via the microRNA.org website (http://www.microrna.org/microrna/home.do). The results indicated that both lncRNA PVT1 and CARM1 can combine with miR-424-5p (Figures 3A and 3B).
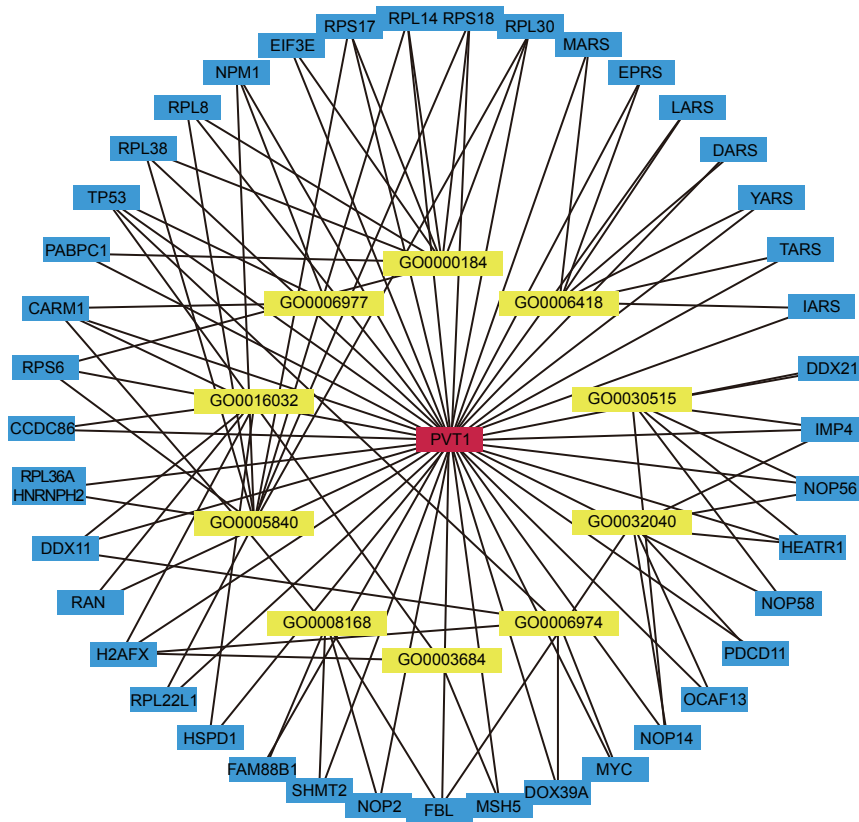
PVT1 expression and radiotherapy-resistant patients had elevated PVT1 expression ($p < 0.05$); PVT1 expression was negatively related to the response of radiotherapy.

A549 and H157 Cell Lines Were Selected for Further Experiments

Our results indicate that PVT1 expression in A460, SPC-A-1, and LTEP-a-2 cell lines was lower than in A549 and H157 cell lines to a great extent. Thus, A549 and H157 cell lines were selected for further experiments (Figure S1).

siRNA-PVT1-1 Was Used as Interference Plasmid

In order to avoid an off-target effect, three kinds of small interfering RNAs (siRNAs) were selected for transfection and to detect silencing efficiency. As Figure S2 displays, after 48 h of transfection, all siRNAs in the A549 and H157 cell lines had remarkably reduced PVT1 expression, and the siRNA-PVT1-1 group had the lowest when compared with the negative control (NC) group ($p < 0.05$), so the siRNA-PVT1-1 was used as the interference plasmid for subsequent experiments.

Short-Term Efficacy of All 80 NSCLC Patients

Among 80 patients, 3 NSCLC patients had a complete response (CR), 44 had a partial response (PR), 19 developed stable disease, and 14 developed progressive disease (PD). Therefore, 47 patients (58.75%) were radiosensitive and the remaining 33 patients (41.25%) were of radiotherapy resistant.

Higher Positive Expression of CARM1 in NSCLC Tissues

CARM1 was detected to express in both the cytoplasm and nucleus, presenting as a dark brown staining particle. Notably, CARM1 expression was higher in NSCLC tissues than in adjacent tissues (Figure 4) ($p < 0.05$).

PVT1 and CARM1 Were Highly Expressed and miR-424-5p Was Lowly Expressed in NSCLC Tissues

As the results showed (Figure 5), NSCLC tissues had increased mRNA and protein expression of PVT1, CARM1, matrix metalloproteinase 2 (MMP-2), and Bcl-2 but decreased expression of miR-424-5p and Bax as compared with adjacent tissues ($p < 0.05$), suggesting that PVT1 and CARM1 were highly expressed and miR-424-5p was lowly expressed in NSCLC tissues.

Negative Relation between PVT1 Expression and NSCLC Radiosensitivity

As Table 1 shows, compared with the PVT1 expression in NSCLC patients before radiotherapy, the radiosensitive patients had reduced

PVT1 Is Verified as the Target Gene of miR-424-5p

As the online predicting software indicated, there was a combination of miR-424-5p (previously named miR-424) and PVT1 3′ untranslated region (3′UTR) (Figure S3A), which verified that PVT1 was the direct target gene of miR-424-5p. Figure S3B shows that, compared with the NC group, the luciferase activity of PVT1-Wt was weakened in the miR-424-5p mimic group while being promoted in the miR-424-5p inhibitor group ($p < 0.05$). But the luciferase activity of the mutant plasmid had no obvious changes ($p > 0.05$). Besides, the results in A549 and H157 tilted toward the same tendency. All of above data suggest that PVT1 can combined with miR-424-5p.

Interaction between PVT1 and CARM1

Figure S4 shows that, compared with the immunoglobulin G (IgG) NC group, PVT1 was expressed higher in the CARM1 antibody group in the A549 and H157 cell lines ($p < 0.05$), which indicated that there was an interaction between PVT1 and CARM1.

siRNA-PVT1 or Overexpressed miR-424-5p Increases Radiosensitivity

Figure S5 shows that differences in cell activity between the blank group and the NC group had no statistical significance ($p > 0.05$).
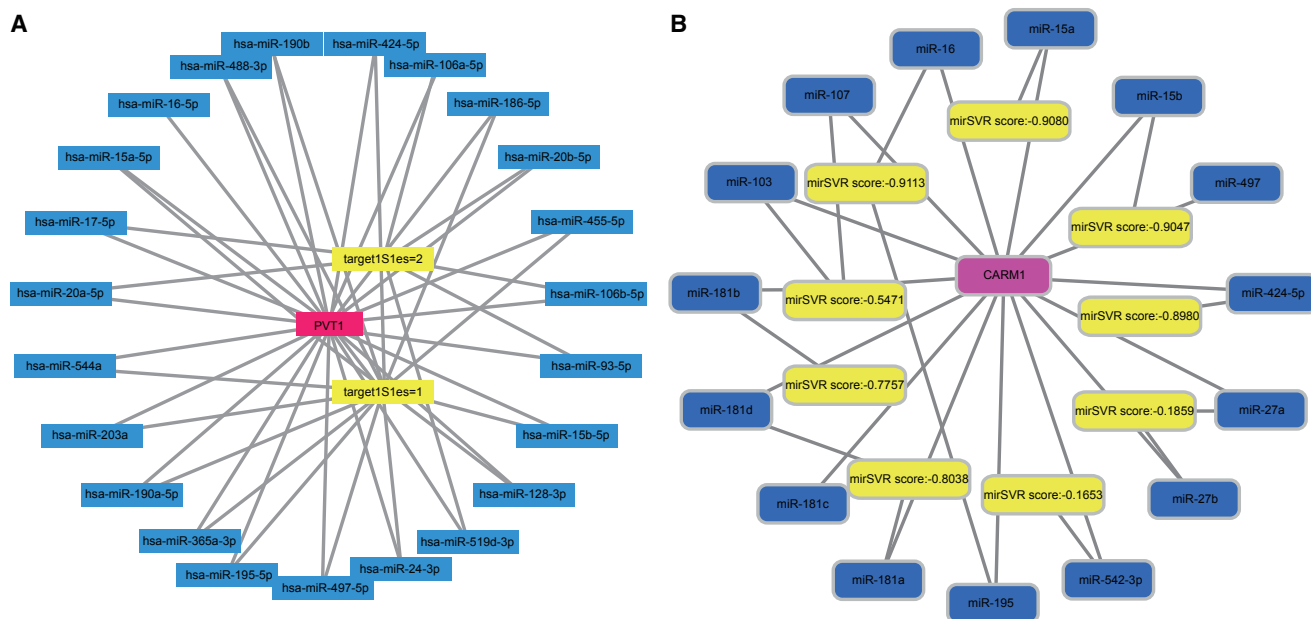
Figure 3. Combined Site of lncRNA PVT1 and miRNA on the Forward of mRNA

(A) PVT1 and (B) CARM1. lncRNA, long non-coding RNA; PVT1, plasmacytoma variant translocation 1; CARM1, co-activator-associated arginine methyltransferase 1.

Compared with the blank and NC groups, the siRNA-PVT1 and miR-424-5p mimic groups had a decreased survival fraction, while the miR-424-5p inhibitor group had an increased survival fraction (p < 0.05). Compared with the miR-424-5p inhibitor group, a reduced survival fraction was found in the siRNA-PVT1 + miR-424-5p inhibitor group (p < 0.05). The same tendency was detected in the A549 and H157 cell lines. Corresponding with the proven negative relation of PVT1 and miR-424-5p, siRNA-PVT1 and overexpressed miR-424-5p increased radiosensitivity; in addition, siRNA-PVT1 can reverse reduced radiosensitivity caused by downregulated miR-424-5p.

siRNA-PVT1 or Overexpressed miR-424-5p Suppressed Expression of CARM1 and Some Other Factors Related to Tumor Progression and Cell Apoptosis

Figure S6 indicates that the A549 and H157 cell lines had a consistent tendency. The NC group had no significant difference when compared with the blank group (p > 0.05). Compared with the blank and NC groups, upregulated expression of miR-424-5p and Bax but downregulated expression of PVT1, CARM1, MMP-2, MMP-9, and Bcl-2 were found in the siRNA-PVT1 and miR-424-5p mimic groups. However, decreased expression of miR-424-5p and Bax and increased expression of PVT1, CARM1, MMP-2, MMP-9, and Bcl-2 were found in the miR-424-5p inhibitor group (p < 0.05). Increased expression of miR-424-5p and Bax and decreased expression of PVT1, CARM1, MMP-2, MMP-9, and Bcl-2 were presented in the siR-PVT1 + miR-424-5p inhibitor group as compared with the miR-424-5p inhibitor group (p < 0.05). These data suggest that siRNA-PVT1 or overexpressed miR-424-5p suppressed the expression of CARM1 and some other factors related to tumor progression and

cell apoptosis. In addition, siRNA-PVT1 can reverse the increased expression of CARM1 and some other factors of tumor progression and cell apoptosis caused by downregulated miR-424-5p.

siRNA-PVT1 or Overexpressed miR-424-5p Inhibits Cell Proliferation

Figure S7 demonstrates that the A549 and H157 cell lines had same tendency of cell proliferation. Differences of cell activity between the blank group and the NC group had no statistical significance (p > 0.05). Compared with the blank and NC groups, the cell proliferation was inhibited in the siRNA-PVT1 and miR-424-5p mimic groups but promoted in the miR-424-5p inhibitor group (all p < 0.05). Moreover, the siR-PVT1 + miR-424-5p inhibitor group had decreased activity of cell growth as compared with the miR-424-5p inhibitor group (p < 0.05). These results suggest that siRNA-PVT1 or overexpressed miR-424-5p suppressed NSCLC cell proliferation, and siRNA-PVT1 reversed elevated proliferation caused by the downregulation of miR-424-5p.

siRNA-PVT1 or Overexpressed miR-424-5p Suppresses Cell Migration and Invasion

Figure S8 shows that the same tendency of cell migration and invasion was confirmed between the A549 and H157 cell lines. Cell migration and invasion in the blank and NC groups had no statistical significance (p > 0.05). Compared with the blank and NC groups, cell migration and invasion were decreased in the siRNA-PVT1 and miR-424-5p mimic groups but increased in the miR-424-5p inhibitor group (all p < 0.05). Cell migration and invasion were promoted in the siRNA-PVT1 + miR-424-5p inhibitor group when compared with the
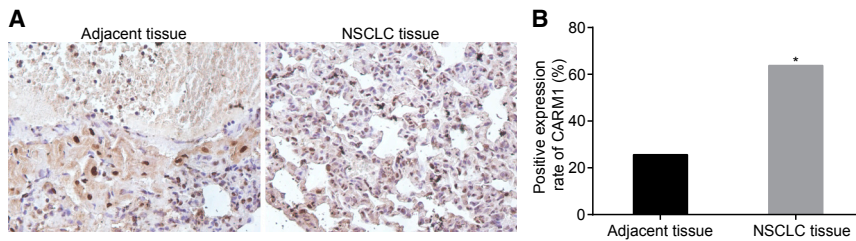
Figure 4. Immunocytochemistry Reveals Higher Positive Expression of CARM1 in NSCLC Tissues (n = 80)

(A) Immunocytochemistry (×400) and (B) CARM1 positive expression. *p < 0.05, compared with the adjacent tissues. NSCLC, non-small cell lung cancer; CARM1, co-activator-associated arginine methyltransferase 1.

miR-424-5p inhibitor group (p < 0.05). It revealed that siRNA-PVT1 or overexpressed miR-424-5p blocked NSCLC cell migration and invasion and siRNA-PVT1 could reverse the cell migration and invasion induced by downregulated miR-424-5p.

siRNA-PVT1 or Overexpressed miR-424-5p Increases Cell Numbers in G0/G1 Phase and Promotes Apoptosis

Figure S9 shows that the same tendency of cell cycle and apoptosis was discovered between the A549 and H157 cell lines. Cell cycle and apoptosis in the blank and NC groups had no statistical significance (p > 0.05). Compared with the blank and NC groups, increased cell apoptosis and cell number in the G0/G1 phase and decreased cell number in S phase were shown in the siRNA-PVT1 and miR-424-5p mimic groups, while reduced cell apoptosis and cell number in the G0/G1 phase and elevated cell number in S phase were detected in the miR-424-5p inhibitor group (all p < 0.05). Elevated cell numbers in the G0/G1 phase, reduced cell numbers in the S phase, and accelerated apoptosis were found in the siR-PVT1 + miR-424-5p inhibitor group as compared with the miR-424-5p inhibitor group (p < 0.05). The above results demonstrate that siRNA-PVT1 or overexpressed miR-424-5p promoted cell apoptosis and that siRNA-PVT1 could reverse the slowed apoptosis due to the downregulated miR-424-5p.

siRNA-PVT1 or Overexpressed miR-424-5p Inhibits Tumor Growth in A549 Cell Lines

The development of tumor progression had no obvious difference between the blank and NC groups (p > 0.05). Compared with the blank and NC groups, the tumor growth was slowed in the siRNA-PVT1 and miR-424-5p mimic groups but faster in the miR-424-5p inhibitor group (all p < 0.05). Tumor growth was blocked in the siRNA-PVT1 + miR-424-5p inhibitor group as compared with the miR-424-5p inhibitor group (p < 0.05). The results suggest that siRNA-PVT1 or overexpressed miR-424-5p could inhibit tumor growth and that siRNA-PVT1 reversed the tumorigenesis resulted from downregulated miR-424-5p (Figure S10).

DISCUSSION

NSCLC accounted for about 80% of lung cancer in sub-classification and was responsible for the top high cancer-related mortality in both males and females.[16,17] In recent years, individualizing systemic anticancer therapy of NSCLC in late age has made great progression.[18] There is evidence that lncRNA PVT1 could be associated with NSCLC treatment because it induced NSCLC cell proliferation.[19]

Our study explored the role of lncRNA PVT1 on NSCLC radiotherapy response via co-expressed CARM1 and co-operated miR-424-5p.

First, we found PVT1, CARM1, MMP-2, MMP-9, and Bcl-2 were upregulated, while miR-424-5p and Bax were downregulated, in NSCLC tissues. It had been reported that PVT1 expression was markedly elevated in NSCLC tissues and its cell lines[10] and that CARM1 was also upregulated in NSCLC tissues.[13] MMPs were believed to have significant roles in tumor progression via regulating the signaling pathways that affect cell viability, invasion, migration, and inflammation.[20] A previous study found the majority of NSCLC patients had high expression of MMP-2 and MMP-9.[21] Bcl-2 was a crucial regulator of cell apoptotic pathways and was confirmed to be overexpressed in a variety of tumors, including NSCLC.[22] There were numerous studies showing that miRs had important roles in cancer treatment, of which miR-424-5p was found to be significantly downregulated in NSCLC tissues.[23] Bax, one of the members in the Bcl-2 family, an early discovered apoptosis-related gene, was found to be lower expressed in NSCLC tissues than in adjacent tissues.[24] The data were consistent with our results, clarifying dysregulation of various tumor-related factors in NSCLC tissues.

We found expression of PVT1, CARM1, MMP-2, MMP-9, and Bcl-2 was decreased, but miR-424-5p and Bax were elevated, in the miR-424-5p mimic and siRNA-PVT1 groups. It had been implied that miR-424, the big family of miR-424-5p, was negatively targeted by PVT1.[25] It had been verified that elevated miR-195, a member of the miR-16/15/195/424/497 family, enhanced the susceptibility of colorectal cancer cells by inhibiting CARM1, thus leading to a chain reaction of increased Bax and decreased Bcl-2.[26,27] Moreover, the knockdown of lncRNA PVT1 weakened Bcl-2 expression by negatively targeting miR-195 in osteosarcoma cells.[28] From another study, we learned the expression of MMP-3, a member of MMPs family like MMP-2 and MMP-9, was negatively associated with miR-152.[29] A former study showed in the lesion of mammary gland, overexpression of miR-424 cluster clearly resulted in the lost expression of Bcl-2.[30] Therefore, the results indicate that siRNA-PVT1 or overexpressed miR-424-5p suppressed the expression of CARM1 and other factors related to tumor progression and cell apoptosis.

Furthermore, inhibited proliferation, migration, and invasion as well as promoted apoptosis of NSCLC cells were found in the miR-424-5p
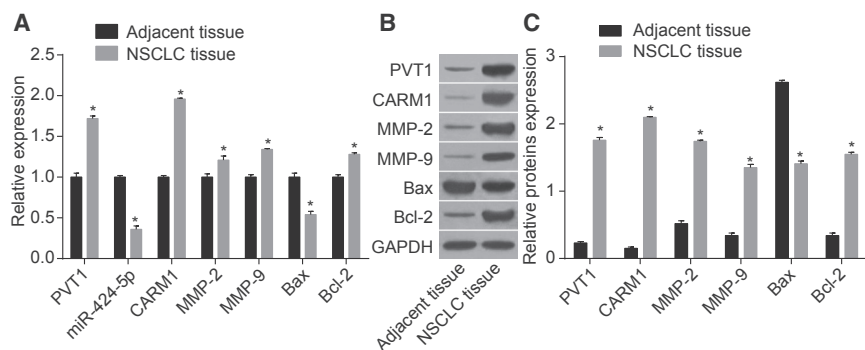
Figure 5. Expression PVT1, miR-424-5p, CARM1, MMP-2, MMP-9, Bcl-2, and Bax in NSCLC (n = 80) and Adjacent Tissues

(A) miR-424-5p expression and mRNA expression of PVT1, CARM1, MMP-2, MMP-9, Bcl-2, and Bax in tissues. (B) Western blot analysis for protein expression. (C) Protein expression of PVT1, CARM1, MMP-2, MMP-9, Bax, and Bcl-2 in tissues. *$p < 0.05$, compared with the adjacent tissues. Data are means ± SD from three independent experiments and analyzed by paired t test. PVT1, plasmacytoma variant translocation 1; miR-424-5p, mircoRNA-424-5p; CARM1, co-activator-associated arginine methyltransferase 1; MMP-2, matrix metallopeptidase-2; MMP-9, matrix metallopeptidase; Bcl-2, B cell lymphoma 2; Bax, Bcl2-associated X protein; NSCLC, non-small cell lung cancer.

mimic and siRNA-PVT1 groups. One previous research study on the association between PVT1 and NSCLC tumorigenesis revealed that siRNA-PVT1 suppressed cell proliferation, migration, and invasion.[11] Also, apoptosis of NSCLC was induced due to the knockdown of PVT1.[19] Correspondingly, researchers also found that PVT1 was higher-expressed in other tumors, such as bladder cancer and thyroid cancer, and that controlling the expression of PVT1 can inhibit cancer cell viability and promote cell apoptosis.[31,32] Similarly, miR-424 inhibited cell invasion and migration but promoted cell apoptosis of glioma cells.[33] What's more, there were observations suggesting that upregulated miR-424 was able to inhibit cell growth via the enhancement of apoptosis and block cell migration and invasion in cervical cancer cell lines.[34] These results suggest siRNA-PVT1 or overexpressed miR-424-5p can inhibit NSCLC cell proliferation, migration, and invasion as well as promote apoptosis.

All in all, our study supports that the knockdown of lncRNA PVT1 and CARM1 as well as the overexpression of miR-424-5p elevates the radiosensitivity of NSCLC. It indeed revealed a novel therapeutic target for tough treatment against NSCLC. But there are still many unknown potential factors affecting the practice of this complicated approach. Therefore, in the future, we will make further efforts to solve these leftover problems.

MATERIALS AND METHODS
Ethical Statement
Informed consent was obtained from all patients, and this study was approved by the Ethical Committee of Chinese PLA General Hospital. All animal experiments were authorized by the local medical committee.

Bioinformatics Prediction
The microarray expression data (GEO: GSE18842 and GSE85716) and annotation probe file relating to NSCLC were downloaded from the GEO database (https://www.ncbi.nlm.nih.gov/geo). These two microarrays were detected by Affymetrix Human Genome U133 Plus 2.0 Array and Agilent-062918 OE Human lncRNA Microarray V4.0 028004, respectively. The Affy installer package of Software

R was adopted for background correction and normalization of microarrays.[35] After that, the linear mode-Bayesian statistics method combined with the traditional t test in the Limma installer package was used to filter nonspecifically for microarray data; in this way, we obtained differentially expressed lncRNA.[36] Differentially expressed lncRNA was predicted by MEM (https://biit.cs.ut.ee/mem/). MEM is a website that provides co-expression queries involving a large number of gene expression experiments. Several hundreds of publicly available gene expression datasets of different kinds of tissue, disease, and condition were allowed to be queried in MEM, which were arranged by the species and microarray platform types.[37] According to the DAVID database (https://david.ncifcrf.gov/), GO analysis was performed in target genes to find out the main biochemical pathway of metabolism that the co-expression gene involved.[38] The starBase database (http://starbase.sysu.edu.cn/index.php) was employed to filter miR that was combined with lncRNA and was able to predict miR-target interactions as well as crosslinking-immunoprecipitation and high-throughput sequencing (CLIP-Seq) data. miR binding to a co-expression gene was filtered via the microRNA.org website (http://www.microrna.org/microrna/home.do).

Study Subjects
Altogether, 80 NSCLC patients admitted to the radiotherapy center of the Chinese PLA General Hospital from January 2014 through October 2016 and were casually selected for this study (59 males and 21 females; 33~72 years old; mean age: 54.64 ± 9.88), with 42 squamous carcinoma and 38 adenocarcinoma. On the basis of the tumor–node–metastasis (TNM) staging criterion of lung cancer set by the Union for International Cancer Control (UICC) in 2009, 49 patients were in stage IIIA and the rest were in stage IIIB. The inclusion criteria were as follows: (1) the patient was diagnosed with NSCLC by clinical method; (2) no relative NSCLC treatment was received in the past 3 months; (3) the Karnofsky performance status (KPS) mark was over 70; (4) the predicted survival time was longer than 3 months.

Evaluation of Radiotherapy Response
Linear accelerator (23EX, Varian Associates, Palo Alto, CA, USA) was employed to classify three-dimensional conformal radiotherapy or

Table 1. The Relation of PVT1 Expression and NSCLC Radiotherapy Response

Response	Cases	PVT1 Expression	p Value
All	80	1.62 ± 0.3	–
CR	3	1.21 ± 0.05	< 0.001
PR	44	1.45 ± 0.18	< 0.001
Stable disease	19	1.77 ± 0.20	< 0.001
PD	14	2.10 ± 0.22	< 0.001

CR, complete response; PR, partial response; PD, progressive disease.

Table 2. Primer Sequences for RT-qPCR

Genes	Primer Sequences
PVT1	F: 5′-TTGGCACATACAGCCATCAT-3′
	R: 5′-GCAGTAAAAGGGGAACACCA-3′
miR-424-5p	F: 5′- CAGCAGCAATTCATGT-3′
	R: 5′- TGGTGTCGTGGAGTCG-3′
U6	F: 5′-GGCTGGTAAGGATGAAGG-3′
	R: 5′-TGGAAGGAGGTCATACGG-3′
CARM1	F: 5′-TTGATGTTGGCTGTGGCTCTGG-3′
	R: 5′-ATGGGCTCCGAGATGATGATGTCC-3′
MMP-2	F: 5′-AGGGCACATCCTATGACAGC–3'
	R: 5′-ATTTGTTGCCCAGGAAAGTG–3'
MMP-9	F: 5′-GCCACCCGAGTGTAACCAT-3′
	R: 5′-TCCCTGGAGACCTGAAACC-3′
Bax	F: 5′-AAGCTGAGCGAGTGTCTCCGGCG-3′
	R: 5′-GCCACAAAGATGGTCACTGTCTGCC-3′
Bcl-2	F: 5′-CTCGTCGCTACCGTCGTGACTTCG-3′
	R: 5′-CAGATGCCGGTTCAGGTACTCAGTC-3′
GAPDH	F: 5′-AGTCCACTG GCGTCTTCA-3′
	R: 5′-GAGTC CTTCCACGATACCAA-3′

miR-424-5p, microRNA-424-5p; CARM1, co-activator-associated arginine methyltransferase 1; MMP-2, matrix metalloproteinase-2; MMP-9, matrix metalloproteinase-9; Bax, Bcl2-associated X protein; Bcl-2, B cell lymphoma-2; GAPDH, glyceraldehyde-3-phosphate dehydrogenase; F, forward; R, reverse.

intensity-modulated radiotherapy. Conventional radiotherapeutic dose was 2 Gy per time, five times per week, with a total dose of 60∼70 Gy/6∼7 weeks. After the whole course of treatment, curative response was evaluated through chest scan. Four kinds of response were classified as the Response Evaluation Criteria in Solid Tumors (RECIST): CR, PR, stable disease, and PD. CR and PR were classified as radiosensitive, while stable disease and PD were considered radiotherapy resistant.

Immunocytochemistry

NSCLC tissues and relative adjacent tissues were extracted via pathological biopsy from the patients before radiotherapy, which were fixed by 4% neutral formalin buffer (DF0113, Beijing Solarbio Science & Technology, Beijing, China), embedded with paraffin, and cut into 4 μm serial sections. After baking at 60°C for 1 h, the sections were dewaxed in xylene (YB-5485, Shanghai Yubo biological technology, Shanghai, China), dehydrated in gradient ethanol, immersed in 3% H_2O_2 at room temperature for 15 min to remove endogenous peroxidase activity, and washed with PBS. After drying, the heat-induced antigen retrieval was conducted two times, and 10% goat serum was added to seal sections for 15 min. Then, the rabbit anti-CARM1 (1:100, bs-4098R, Beijing Bioss biotechnology, Beijing, China) primary antibody was added for incubation at 4°C overnight and the sections were washed with PBS three times. Biotin-labeled secondary goat anti-rabbit IgG (1:1,000, ab6721, Abcam, Cambridge, MA, USA) was subsequently added for incubation at 37°C for 40 min and the sections were washed by PBS. The samples were stained with diaminobenzidine (DAB) (DA1010, Beijing Solarbio Science & Technology, Beijing, China) for 10 min, re-stained with hematoxylin (H8070, Beijing Solarbio Science & Technology, Beijing, China) for 1 min, and washed by running water, dehydrated with alcohol, cleared by xylene, and sealed with neutral balsam. The primary antibody was replaced with PBS, which was taken as NC. The final result was evaluated by double-blind method. Five fields of high power under an optical microscope (CX41-12C02, Olympus Optical, Tokyo, Japan) were selected by chance. The appearance of dark brown staining particle in the cell was a sign of a positive cell. The CARM1 protein staining results relied on the quantity of positive cells accounting for the total quantity of cells: the positive expression (+) was represented by the ratio over 10%; otherwise, the negative expression (-) was presented.

qRT-PCR

The total RNA of NSCLC cells and tissues were extracted with Trizol kits (No: 15596026, Invitrogen, Carlsbad, CA, USA) by one-step method, and miRNA was extracted with mirVanaTM miRNA kits (AM1552, Ambion, Austin, TX, USA). The concentration and purity of RNA were tested by UV spectrophotometry (DU640, Beckman Coulter, Chaska, MN, USA), and high purity was marked by a A260/A280 ratio ranging from 1.8∼2.0. As the instructions of PrimeScript RT reagent kit (RR047A, Takara Holdings Inc., Kyoto, Japan) indicated, RNA was reversely transcribed into cDNA. A SYBR Premix EX Taq kit (RR420A, Takara Holdings, Kyoto, Japan) was used to conduct PCR reaction by a qRT-PCR instrument (ABI7500, ABI, Oyster Bay, NY, USA). The reaction system was as follows: 9 μL SYBR Mix, 0.5 μL forward primer, 0.5 μL reverse primer, 2 μL cDNA, and 8 μL RNase-free double-distilled water (ddH2O). The corresponding reactive condition was at 95°C for 10 min, 95°C for 15 s, and 60°C for 1 min, respectively, for 40 continuous cycles. Three duplicated wells were made for each sample. PVT1, miR-424-5p, CARM1, MMP-2, MMP-9, Bcl2-associated X protein (Bax), B cell lymphoma 2 (Bcl-2), U6, and glyceraldehyde-3-phosphate dehydrogenase (GAPDH) primers were all synthesized by Shanghai Genechem (Shanghai, China) (Table 2). U6 was used as the internal reference for control expression of miR-424-5p, and GAPDH was seen as the internal reference of PVT1, CARM1, MMP-2, MMP-9, Bax, Bcl-2, with the cycle threshold

Table 3. Primer Sequences for Transfection

Groups	Sequences
miR-424-5p mimic	5′-CAGCAGCAAUUCAUGUUUUGAA-3′
	5′- CAAAACAUGAAUUGCUGCUGUU-3
miR-424-5p inhibitor	5′-UUCAAAACAUGAAUUGCUGCUG-3′
	5′-CAGUACUUUUGUGUAGUACAA-3′
NC	5′-UUCUCCGAACGUGUCACGUTT-3′
	5′-ACGUGACACGUUCGGAGAATT-3′
siRNA-PVT1-1	5′-GCUUCUCCUGUUGCUGCUATT-3′
	5′-UAGCAGCAACAGGAGAAGCTT-3′
siRNA-PVT1-2	5′-GCUUGGAGGCUGAGGAGUUTT-3′
	5′-AACUCCUCAGCCUCCAAGCTT-3′
siRNA-PVT1-3	5′-AAGGAAGCUCUUCUUGAGC-3
	5′-GCUC AAGAAGAGCUUCCUU-3′

miR-424-5p, microRNA-424-5p; PVT1, plasmacytoma variant translocation 1; NC, negative control.

(Ct) value in each well recorded. The $2^{-\Delta\Delta Ct}$ method was adopted to calculate relative levels of target genes: $\Delta\Delta Ct = (\Delta Ct_{\text{target gene}} - \Delta Ct_{\text{housekeeping gene}}) - (\Delta Ct_{\text{target gene}} - \Delta Ct_{\text{housekeeping gene}})$. The experiment was repeated thre times to obtain mean value.

Western Blot Analysis

The total protein in tissues and cells was extracted using radioimmunoprecipitation assay (RIPA) lysis buffer containing phenylmethanesulfonyl fluoride (PMSF) (R0010, Beijing Solarbio Science & Technology, Beijing, Shanghai). After incubation on ice for 30 min, the samples were centrifuged at 4°C and 25,764 g for a total of 10 min with supernatant collected. The protein concentration of each sample was measured by bicinchoninic acid (BCA) kit and adjusted with deionized water. Then a 10% SDS-PAGE (P0012A, Beyotime Biotechnology, Shanghai, China) was configured for protein separation. After that, the protein was transferred to polyvinylidene fluoride (PVDF) membrane (ISEQ00010, Millipore, Billerica, MA, USA) under 110 V for 2 h. The PVDF membrane was added with Tris-buffered saline tween (TBST) containing 5% dried skimmed milk for 2 h. After the buffer was removed, the samples were washed one time with TBST, added with the primary antibody rabbit anti-CARM1 (1:100, bs-4098R, Beijing Bioss biotechnology, Beijing, China), rabbit anti-MMP-9 (1:100, bs-4599R, Beijing Bioss biotechnology, Beijing, China), rabbit anti-Bcl-2 (1:100, bs-4563R, Beijing Bioss biotechnology, Beijing, China), and rabbit anti-GAPDH (1:2,500, ab9485, Abcam, Cambridge, MA, USA) for incubation at 4°C overnight and finally washed with TBST three times (10 min for each time). After the addition of horseradish peroxidase-labeled goat anti-rabbit IgG secondary antibody (1:2,000, ab6721, Abcam, Cambridge, MA, USA), the samples were incubated at room temperature for 1 h and washed three times with PBS tween-20 (PBST) (10 min each time). The membrane was immersed in enhanced chemiluminescence (ECL) reaction solution (WBKLS0100, Millipore, Billerica, MA, USA) to develop colors and then develop images after exposure in the darkness. Taking the GAPDH as internal control, the ratio of gray value between target protein bands and internal control bands was regarded as the relative level. The experiment was repeated three times to obtain mean value.

Cell Culture

Five common NSCLC cell lines, A549, H460, H1299, SPC-A-1, and LTEP-A-2 (ATCC, Manassas, VA, USA), were selected for this experiment. After recovery, the cell lines were cultivated in an incubator (BB15, Thermo Fisher Scientific, Waltham, MA, USA) of saturated humidity with 5% CO_2 at 37°C with DMEM (No. 12800017, GIBCO, Grand Island, NY, USA) containing 10% fetal bovine serum (FBS) (No. 26140079, GIBCO, Grand Island, NY, USA). Cell passage was conducted when the cell confluence reached 90%. The culture solution was removed and the cells were washed twice with PBS. Until the cells were isolated into single-cell and presented in round shape after the detachment with 0.25% trypsin, DMEM containing 10% FBS was added to terminate digestion. A transfer liquid gun was employed to percuss the cells to single-cell suspension. The expression of PVT1 in these five cell lines was detected by qRT-PCR, and the highest two were to be used in later experiments.

Cell Grouping and Transfection

The NSCLC cells were allocated into a blank group (no transfection), NC group (transfected with blank plasmid), siRNA-PVT1 group (transfected with the most silenced siRNA-PVT1 plasmid of the selected three), miR-424-5p mimic group (transfected with miR-424-5p mimic plasmid), miR-424-5p inhibitor group (transfected miR-424-5p inhibitor plasmid), and siRNA-PVT1 + miR-424-5p inhibitor group (co-transfected with siRNA-PVT1 and miR-424-5p inhibitor plasmid). The target plasmids were all purchased from Dharmacon (Lafayette, CO, USA). Subsequently, the NSCLC cells were seeded into a 6-well plate (3×10^5 cells/well). A Lipofectamine 2000 kit (Invitrogen Inc., Carlsbad, CA, USA) was used to transfect when the cell confluence was up to 90%. Next, 250 μL serum-free Opti-MEM (GIBCO, Grand Island, NY, USA) was used to dilute 4 μg target plasmid and 10 μL of Lipofectamine 2000, respectively, with light mixture. Standing at room temperature for 5 min, the two were mixed evenly and added to the culture well before twice standing for 20 min, which were then cultured in a 5% CO_2 incubator at 37°C for 6 h. After that, the complete culture medium was used for further culturing. After 48 h culture, the cells were collected for further use. The sequences are shown in Table 3.

Dual Luciferase Reporter Assay

The website microRNA.org was used to predict the target gene of miR-424-5p. The PVT1 3′UTR sequence was amplified via PCR. Double enzyme digestion of the restriction sites Xho I and Not I was conducted in order to clone the target fragments into the reverse of luciferase reporter gene pmirGLO (No. 3577193, Promega, Madison, WI, USA), named pPVT1-wide type (pPVT1-Wt), which was prepared for later use after being picked and purified. Next, site-specific mutagenesis was conducted for the combined site of miR-424-5p

and PVT1, and pPVT1 mutant (pPVT1-Mut) vector was constructed. pPVT1-Wt and pPVT1-Mut were co-transfected with the NC, miR-424-5p mimic, or miR-424-5p inhibitor into the A549 cells. After transfection for 24 h, the cells were split and centrifuged at 12,000 rpm for 1 min with supernatant collected. The luciferase activity was measured by the Dual-Luciferase Reporter Assay System (E1910, Promega, Madison, WI, USA). Finally, each sample was added with 100 μL firefly luciferase fluid to detect firefly luciferase and 100 μL ranilla luciferase fluid to detect ranilla luciferase. The ratio between firefly luciferase and ranilla luciferase was regarded as relative luciferase activity. This experiment was repeated three times.

RIP Assay

An RNA immunoprecipitation (RIP) kit (No. 17-701, Millipore, Billerica, MA, USA) was employed to ensure the combination of PVT1 and CARM1. NSCLC cells were collected, washed twice with precooled PBS, and centrifuged at 4°C and 402 g for 5 min with supernatant removed. RIP lysate in the same volume was used for cell-resuspend with light mixture. Following the ice bath for 5 min, the samples were separately reserved at −80°C. After fully resuspended, 50 μL magnetic bead suspension was taken into an eppendorf (EP) tube. Then, 500 μL RIP wash buffer was added to mix vortically. The EP tube was stored at the magnet base and turned left and right until the magnetic beads gathered and lined up before the supernatant was removed. The procedure was repeated again. Next, 100 μL RIP wash buffer was added to re-suspend the magnetic bead and 5 μg rabbit anti-CARM1 antibody (1: 20, PA5-17304, Thermo Fisher Scientific, Waltham, MA, USA) was added and mixed evenly at room temperature for 30 min. The IgG antibody was taken as the NC. The EP tube was placed in the magnet base to remove the supernatant. After the addition of 500 μL RIP wash buffer, the samples were vortically mixed with supernatant removed and then a repetition was required. Subsequently, 900 μL RIP buffer was added after the EP tube was placed on the magnet base with supernatant removed. The cell lysate was thawed and centrifuged at 4°C and 14,000 rpm for 10 min. 100 μL supernatant was added to the prepared magnetic bead suspension to incubate with 1 mL of the system. 10 μL cell lysate supernatant was taken as RNA input, reserved at −80°C, shaken at 4°C, and incubated overnight. After transient centrifugation, the samples were put in the magnet base with supernatant removed. With the addition of 500 μL RIP wash buffer and even mixture, these samples were stored at the magnet base with supernatant removed, which required five repetitions. After digestion with 150 μL protease K, RNA was extracted, and the expression of PVT1 in the CARM1 antibody group, IgG NC group, and input group was tested by qRT-PCR to make a comparison.

Clonogenic Assay

The transfected cells in the logarithmic growth phase of all six groups were detached by 0.25% trypsin and percussed to single-cell suspension by transfer liquid gun. After centrifugation, DMEM solution containing 10% FBS was used to terminate digestion. Following the cell accounting with a counting plate, the cells in different quantity (200, 200, 400, 2,000, and 4,000 cells/well) were continually incubated into the 6-well plate, respectively, according to the different exposure dose (0, 2, 4, 6, and 8 Gy), and culture medium was added until 3 mL/well in each well was reached. Then the 6-well plate was lightly shaken in a cross direction to make the cells disperse evenly and then cultured in a 5% CO_2 incubator at 37°C for a week, with solution substituted in every 2 days. When the clone lump could be seen in the bottom, the culture was stopped, and the solution was removed. The plate was washed twice by PBS, 2 mL methanol was added and left for 20 min to fix the cells, and then the methanol was removed. 2 mL Giemsa staining liquor (G4640, Beijing Solarbio Science & Technology, Beijing, China) was used to stain the cells for 40 min, which was then washed away by distilled water. The plate was placed for aeration drying. An inverted microscope (IX-50, Olympus Optical, Tokyo, Japan) was used to record the valid clone quantity (over 50 cells). Cloning efficiency (CE) = the clone formation quantity (at 0 Gy dose)/cell incubation number × 100%, and the survival fraction (SF) = the clone-formation quantity after exposure/(cell incubation number × CE) × 100%.

Cell Counting Kit-8 Assay

The transfected cells in the logarithmic growth phase of all six groups were washed twice with PBS, treated by 0.25% trypsin, then centrifuged (at 178 g for 5 min), and subsequently percussed to well-distributed single-cell suspension with transfer liquid gun. The cells were seeded into a 96-well plate (2.5×10^3 cells in each well) and cultured in a 5% CO_2 incubation at 37°C. Each well had four repetitions. After 24 h, cell counting kit-8 (CCK-8) reagent (CK04, Dojindo Laboratories, Kumamoto, Japan) was added to the plate (10 μL/well). After the mixed well, the cells were cultured again in a 5% CO_2 incubator at 37°C for 2 h. The optical density (OD) value of wells was detected at 450 nm using an automatic enzyme-mark reader (Multiskan FC, Thermo Fisher Scientific, Waltham, MA, USA) for 3 days. The cell growth curve was drawn with the x axis referring to time and the y axis representing mean OD value to measure cell activity.

Scratch Assay

A marker pen was used to draw lines evenly at the back of the 6-well plate, with three transverse lines crossed over each well. The NSCLC cells of all six groups in logarithmic growth phase were seeded into a 6-well plate (5×10^5 cells in each well). After culture for 24 h, when the cells covered the whole plate, a 200 μL transfer liquid gun was used to draw lines perpendicular to the transverse lines at the back of the plate. Every three vertical lines crossed over each well. PBS was used to wash away the scratched cells. Serum-free DMEM was added to the plate that was cultured in a 5% CO_2 incubator at 37°C. Then, at 0 h and 24 h, samples were taken and photographed by the inverted microscope (three parallel wells in each group). The cell migration ability was tested.

Transwell Assay

The NSCLC cells in the logarithmic growth phase were digested by trypsin, centrifuged (at 28 g for 5 min) at room temperature with supernatant removed, washed one time with PBS, and added with serum-free DMEM to resuspend the cells. The cell density was

adjusted to 5×10^5 cells/mL. A total of 200 μL suspension was added to the upper Transwell chamber (No. 3414, Millipore, Billerica, MA, USA) coated with matrigel (about 3×10^5 cells in each well). 0.6 mL DMEM containing 30% FBS was added to the bottom chamber. With three duplicated wells in each group, the chamber was cultured in a 5% CO_2 incubator at 37°C for 48 h. After that, the cells were fixed by 4% paraformaldehyde for 20 min and stained by 0.1% crystal violet for 30 min, with dye liquor washed off by PBS. When it was dried by airing, five fields were randomly selected to count the cell number using an inverted microscope, and the mean value was obtained. This experiment was conducted three times. The number of cells passed through the matrigel referred to the ability of cell invasion.

Flow Cytometry
The transfected cells of all six groups in the logarithmic growth phase were detached by 0.25% trypsin. Cells were seeded into a 6-well plate and cultured for 48 h with cell density adjusted to 3×10^5/mL. After being washed by PBS twice, single-cell suspension was generated and then centrifuged at 178 g for 5 min with supernatant removed. Next, the cells were fixed by 70% cold ethanol at $-20°C$ for 1 h and centrifuged again at 178 g for 5 min with supernatant removed. Next, 200 μL pre-cooling PBS was added to wash cells twice. 20 μL RNA enzyme was added at 37°C for 30 min to create a reaction. 400 μL propidium iodide (PI) (C0080, Beijing Solarbio Science & Technology, Beijing, China) was added and incubated on ice in the dark for 15 min. Flow cytometry (BDLSR II, Becton, Dickinson and Company, NJ, USA) was employed to detect cell cycles using 488 nm excitation. The cells were washed twice by pre-cooling PBS and centrifuged at 1,000 r·min^{-1} for 5 min, with supernatant removed so as to detect cell apoptosis. 400 μL Annexin V binding buffer (CA1020, Beijing Solarbio Science & Technology, Beijing, China) was used to resuspend cells (3×10^5/mL) that centrifuged at 178 g for 5 min with supernatant removed. With the addition of 50 μL Annexin-V-fluorescein isothiocyanate (Annexin-V-FITC), the cells were incubated on ice in the darkness for 15 min and added with 10 μL of PI to have a reaction in the darkness for 5 min after mixed. The cell apoptosis was tested using 488 nm excitation. The experiment was repeated three times with the mean value required.

Tumorigenicity Assay in Nude Mice
The A549 cells in the logarithmic growth phase (5×10^6 cells in each group) in six groups were injected subcutaneously into the back of the female BALB/c nude mice (4–6 weeks old). As the tumor volume reached 50 mm^3, the mice were exposed to 8 Gy X-ray. After that, the tumor volume ($0.5 \times$ length $\times$ width) was recorded every 5 days, and the tumor graph was drawn. At the 21st day after X-ray, the mice were sacrificed to separate the tumor, and the tumor weight was measured.

Statistical Analysis
SPSS 21.0 (IBM, Armonk, NY, USA) was used to process the data. All experiments were conducted three times. The measurement data were expressed as mean ± SD. Differences between two groups were compared by t test and differences among multiple groups were analyzed by single-factor variance analysis. $p < 0.05$ was considered statistically significant.

AUTHOR CONTRIBUTIONS
D.W. designed the study. H.Y. collated the data, designed and developed the database, carried out data analyses, and produced the initial draft of the manuscript. All authors contributed to drafting the manuscript. All authors have read and approved the final submitted manuscript.

CONFLICTS OF INTEREST
The authors declare no competing interests.

REFERENCES
1. Santos, F.N., de Castria, T.B., Cruz, M.R., and Riera, R. (2015). Chemotherapy for advanced non-small cell lung cancer in the elderly population. Cochrane Database Syst. Rev. (10), CD010463.

2. Reck, M., Heigener, D.F., Mok, T., Soria, J.C., and Rabe, K.F. (2013). Management of non-small-cell lung cancer: recent developments. Lancet 382, 709–719.

3. Jang, I., Jeon, B.T., Jeong, E.A., Kim, E.J., Kang, D., Lee, J.S., Jeong, B.G., Kim, J.H., Choi, B.H., Lee, J.E., et al. (2012). Pak1/LIMK1/Cofilin Pathway Contributes to Tumor Migration and Invasion in Human Non-Small Cell Lung Carcinomas and Cell Lines. Korean J. Physiol. Pharmacol. 16, 159–165.

4. Velcheti, V., Schalper, K.A., Carvajal, D.E., Anagnostou, V.K., Syrigos, K.N., Sznol, M., Herbst, R.S., Gettinger, S.N., Chen, L., and Rimm, D.L. (2014). Programmed death ligand-1 expression in non-small cell lung cancer. Lab. Invest. 94, 107–116.

5. Reck, M., Popat, S., Reinmuth, N., De Ruysscher, D., Kerr, K.M., and Peters, S.; ESMO Guidelines Working Group (2014). Metastatic non-small-cell lung cancer (NSCLC): ESMO Clinical Practice Guidelines for diagnosis, treatment and follow-up. Ann. Oncol. 25 (Suppl 3), iii27–iii39.

6. Toschi, L., and Cappuzzo, F. (2010). Impact of biomarkers on non-small cell lung cancer treatment. Target. Oncol. 5, 5–17.

7. Sellmann, L., Fenchel, K., and Dempke, W.C. (2015). Improved overall survival following tyrosine kinase inhibitor treatment in advanced or metastatic non-small-cell lung cancer-the Holy Grail in cancer treatment? Transl. Lung Cancer Res. 4, 223–227.

8. Wang, L., Chen, Z., An, L., Wang, Y., Zhang, Z., Guo, Y., and Liu, C. (2016). Analysis of Long Non-Coding RNA Expression Profiles in Non-Small Cell Lung Cancer. Cell. Physiol. Biochem. 38, 2389–2400.

9. Zhang, A., Xu, M., and Mo, Y.Y. (2014). Role of the lncRNA-p53 regulatory network in cancer. J. Mol. Cell Biol. 6, 181–191.

10. Cui, D., Yu, C.H., Liu, M., Xia, Q.Q., Zhang, Y.F., and Jiang, W.L. (2016). Long non-coding RNA PVT1 as a novel biomarker for diagnosis and prognosis of non-small cell lung cancer. Tumour Biol. 37, 4127–4134.

11. Yang, Y.R., Zang, S.Z., Zhong, C.L., Li, Y.X., Zhao, S.S., and Feng, X.J. (2014). Increased expression of the lncRNA PVT1 promotes tumorigenesis in non-small cell lung cancer. Int. J. Clin. Exp. Pathol. 7, 6929–6935.

12. Takahashi, Y., Sawada, G., Kurashige, J., Uchi, R., Matsumura, T., Ueo, H., Takano, Y., Eguchi, H., Sudo, T., Sugimachi, K., et al. (2014). Amplification of PVT-1 is

involved in poor prognosis via apoptosis inhibition in colorectal cancers. Br. J. Cancer *110*, 164–171.

13. Elakoum, R., Gauchotte, G., Oussalah, A., Wissler, M.P., Clément-Duchêne, C., Vignaud, J.M., Guéant, J.L., and Namour, F. (2014). CARM1 and PRMT1 are dysregulated in lung cancer without hierarchical features. Biochimie *97*, 210–218.

14. Wang, F., Wang, J., Yang, X., Chen, D., and Wang, L. (2016). MiR-424-5p participates in esophageal squamous cell carcinoma invasion and metastasis via SMAD7 pathway mediated EMT. Diagn. Pathol. *11*, 88.

15. Wang, Y., Lv, Z., Fu, J., Wang, Z., Fan, Z., and Lei, T. (2017). Endogenous microRNA-424 predicts clinical outcome and its inhibition acts as cancer suppressor in human non-small cell lung cancer. Biomed. Pharmacother. *89*, 208–214.

16. Kanaan, Z., Kloecker, G.H., Paintal, A., and Perez, C.A. (2015). Novel targeted therapies for resistant ALK-rearranged non-small-cell lung cancer: ceritinib and beyond. OncoTargets Ther. *8*, 885–892.

17. Kim, M.K., Jung, S.B., Kim, J.S., Roh, M.S., Lee, J.H., Lee, E.H., and Lee, H.W. (2014). Expression of microRNA miR-126 and miR-200c is associated with prognosis in patients with non-small cell lung cancer. Virchows Arch. *465*, 463–471.

18. Cufer, T., Ovcaricek, T., and O'Brien, M.E. (2013). Systemic therapy of advanced non-small cell lung cancer: major-developments of the last 5-years. Eur. J. Cancer *49*, 1216–1225.

19. Wan, L., Sun, M., Liu, G.J., Wei, C.C., Zhang, E.B., Kong, R., Xu, T.P., Huang, M.D., and Wang, Z.X. (2016). Long Noncoding RNA PVT1 Promotes Non-Small Cell Lung Cancer Cell Proliferation through Epigenetically Regulating LATS2 Expression. Mol. Cancer Ther. *15*, 1082–1094.

20. Schveigert, D., Cicenas, S., Bruzas, S., Samalavicius, N.E., Gudleviciene, Z., and Didziapetriene, J. (2013). The value of MMP-9 for breast and non-small cell lung cancer patients' survival. Adv. Med. Sci. *58*, 73–82.

21. Shao, W., Wang, W., Xiong, X.G., Cao, C., Yan, T.D., Chen, G., Chen, H., Yin, W., Liu, J., Gu, Y., et al. (2011). Prognostic impact of MMP-2 and MMP-9 expression in pathologic stage IA non-small cell lung cancer. J. Surg. Oncol. *104*, 841–846.

22. Anagnostou, V.K., Lowery, F.J., Zolota, V., Tzelepi, V., Gopinath, A., Liceaga, C., Panagopoulos, N., Frangia, K., Tanoue, L., Boffa, D., et al. (2010). High expression of BCL-2 predicts favorable outcome in non-small cell lung cancer patients with non squamous histology. BMC Cancer *10*, 186.

23. Zhang, M., Zeng, J., Zhao, Z., and Liu, Z. (2017). Loss of MiR-424-3p, not miR-424-5p, confers chemoresistance through targeting YAP1 in non-small cell lung cancer. Mol. Carcinog. *56*, 821–832.

24. Sun, Q., Hua, J., Wang, Q., Xu, W., Zhang, J., Zhang, J., Kang, J., and Li, M. (2012). Expressions of GRP78 and Bax associate with differentiation, metastasis, and apoptosis in non-small cell lung cancer. Mol. Biol. Rep. *39*, 6753–6761.

25. Gao, Y.L., Zhao, Z.S., Zhang, M.Y., Han, L.J., Dong, Y.J., and Xu, B. (2017). Long Noncoding RNA PVT1 Facilitates Cervical Cancer Progression via Negative Regulating of miR-424. Oncol. Res. *25*, 1391–1398.

26. Wang, X., Wang, J., Ma, H., Zhang, J., and Zhou, X. (2012). Downregulation of miR-195 correlates with lymph node metastasis and poor prognosis in colorectal cancer. Med. Oncol. *29*, 919–927.

27. Zheng, L., Chen, J., Zhou, Z., and He, Z. (2017). miR-195 enhances the radiosensitivity of colorectal cancer cells by suppressing CARM1. OncoTargets Ther. *10*, 1027–1038.

28. Zhou, Q., Chen, F., Zhao, J., Li, B., Liang, Y., Pan, W., Zhang, S., Wang, X., and Zheng, D. (2016). Long non-coding RNA PVT1 promotes osteosarcoma development by acting as a molecular sponge to regulate miR-195. Oncotarget *7*, 82620–82633.

29. Zheng, X., Chopp, M., Lu, Y., Buller, B., and Jiang, F. (2013). MiR-15b and miR-152 reduce glioma cell invasion and angiogenesis via NRP-2 and MMP-3. Cancer Lett. *329*, 146–154.

30. Llobet-Navas, D., Rodríguez-Barrueco, R., Castro, V., Ugalde, A.P., Sumazin, P., Jacob-Sendler, D., Demircan, B., Castillo-Martín, M., Putcha, P., Marshall, N., et al. (2014). The miR-424(322)/503 cluster orchestrates remodeling of the epithelium in the involuting mammary gland. Genes Dev. *28*, 765–782.

31. Zhou, Q., Chen, J., Feng, J., and Wang, J. (2016). Long noncoding RNA PVT1 modulates thyroid cancer cell proliferation by recruiting EZH2 and regulating thyroid-stimulating hormone receptor (TSHR). Tumour Biol. *37*, 3105–3113.

32. Zhuang, C., Li, J., Liu, Y., Chen, M., Yuan, J., Fu, X., Zhan, Y., Liu, L., Lin, J., Zhou, Q., et al. (2015). Tetracycline-inducible shRNA targeting long non-coding RNA PVT1 inhibits cell growth and induces apoptosis in bladder cancer cells. Oncotarget *6*, 41194–41203.

33. Jin, C., Li, M., Ouyang, Y., Tan, Z., and Jiang, Y. (2017). MiR-424 functions as a tumor suppressor in glioma cells and is down-regulated by DNA methylation. J. Neurooncol. *133*, 247–255.

34. Xu, J., Li, Y., Wang, F., Wang, X., Cheng, B., Ye, F., Xie, X., Zhou, C., and Lu, W. (2013). Suppressed miR-424 expression via upregulation of target gene Chk1 contributes to the progression of cervical cancer. Oncogene *32*, 976–987.

35. Fujita, A., Sato, J.R., Rodrigues, Lde.O., Ferreira, C.E., and Sogayar, M.C. (2006). Evaluating different methods of microarray data normalization. BMC Bioinformatics *7*, 469.

36. Smyth, G.K. (2004). Linear models and empirical bayes methods for assessing differential expression in microarray experiments. Stat Appl Genet Mol Biol. *3*, Article3.

37. Adler, P., Kolde, R., Kull, M., Tkachenko, A., Peterson, H., Reimand, J., and Vilo, J. (2009). Mining for coexpression across hundreds of datasets using novel rank aggregation and visualization methods. Genome Biol. *10*, R139.

38. Huang, W., Sherman, B.T., and Lempicki, R.A. (2009). Bioinformatics enrichment tools: paths toward the comprehensive functional analysis of large gene lists. Nucleic Acids Res. *37*, 1–13.

Supplemental Information

Long Non-coding RNA PVT1 Competitively Binds

MicroRNA-424-5p to Regulate CARM1 in

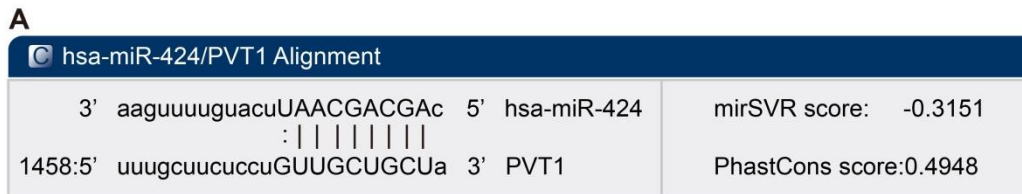# Radiosensitivity of Non-Small-Cell Lung Cancer

Dong Wang and Yi Hu
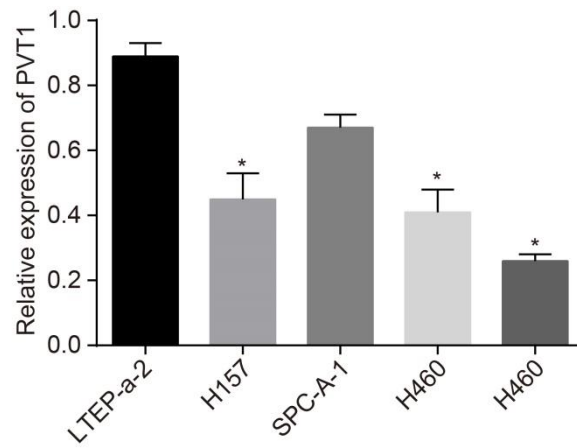
Supplementary Figure 1. Relative expression of PVT1 in five different NSCLC cell lines, and A549 and H157 cells were selected for the following experiment

Note: [*], $P < 0.05$, compared with A549 and H157 cell lines. Data are means ± standard deviation from three independent experiments, P calculated by one way ANOVA; PVT1, plasmacytoma variant translocation 1; NSCLC, non-small cell lung cancer.
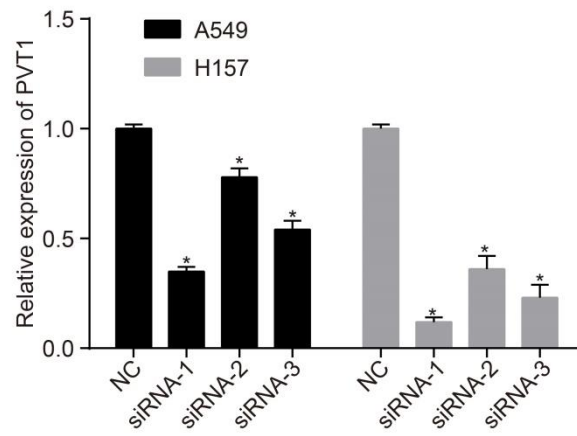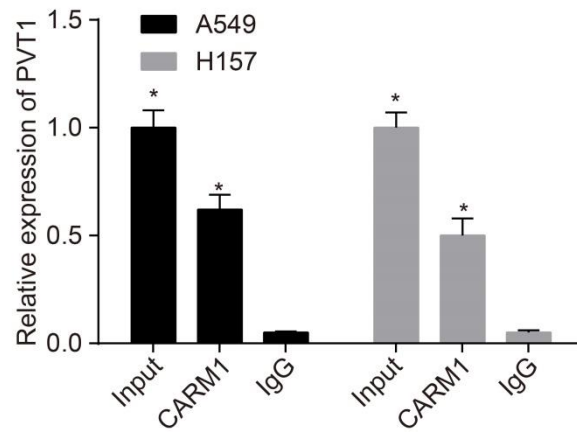
Supplementary Figure 2. The siRNA-1 was selected for the following experiments

Note: *, $P < 0.05$, compared with the NC group; Data are means ± standard deviation from three independent experiments, P calculated by one way ANOVA; PVT1, plasmacytoma variant translocation 1.

A

hsa-miR-424/PVT1 Alignment

3' aaguuuuguacuUAACGACGAc 5' hsa-miR-424 : | | | | | | | | 1458:5' uuugcuucuccuGUUGCUGCUa 3' PVT1	mirSVR score: -0.3151 PhastCons score:0.4948

Mouseover a miRNA mature name to see the miRNA/PVT1 alignment.

B
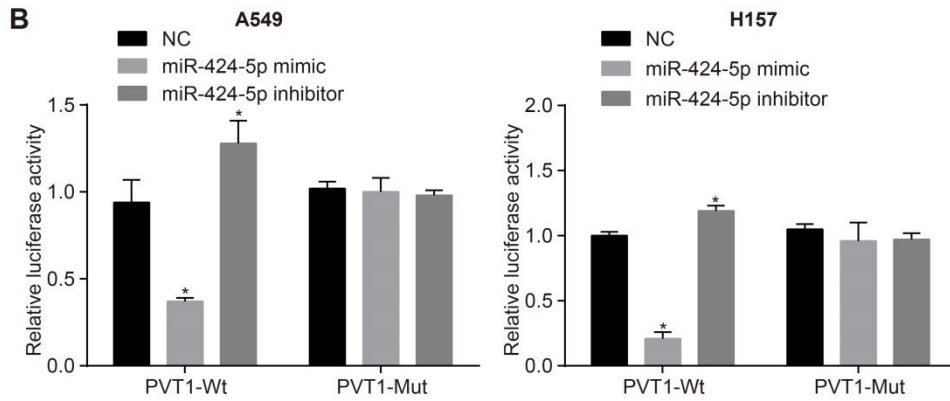
Supplementary Figure 3. PVT1 is verified as the target gene of miR-424-5p

Note: A, combined site of miR-424-5p and PVT1 3' UTR; B, dual luciferase reporter assay of gene activity; *, $P < 0.05$, compared with the NC group; Data are means ± standard deviation from three independent experiments, P calculated by one way ANOVA; miR-424-5p, mircoRNA-424-5p; PVT1, plasmacytoma variant translocation 1; 3' UTR, 3' Untranslated Regions.
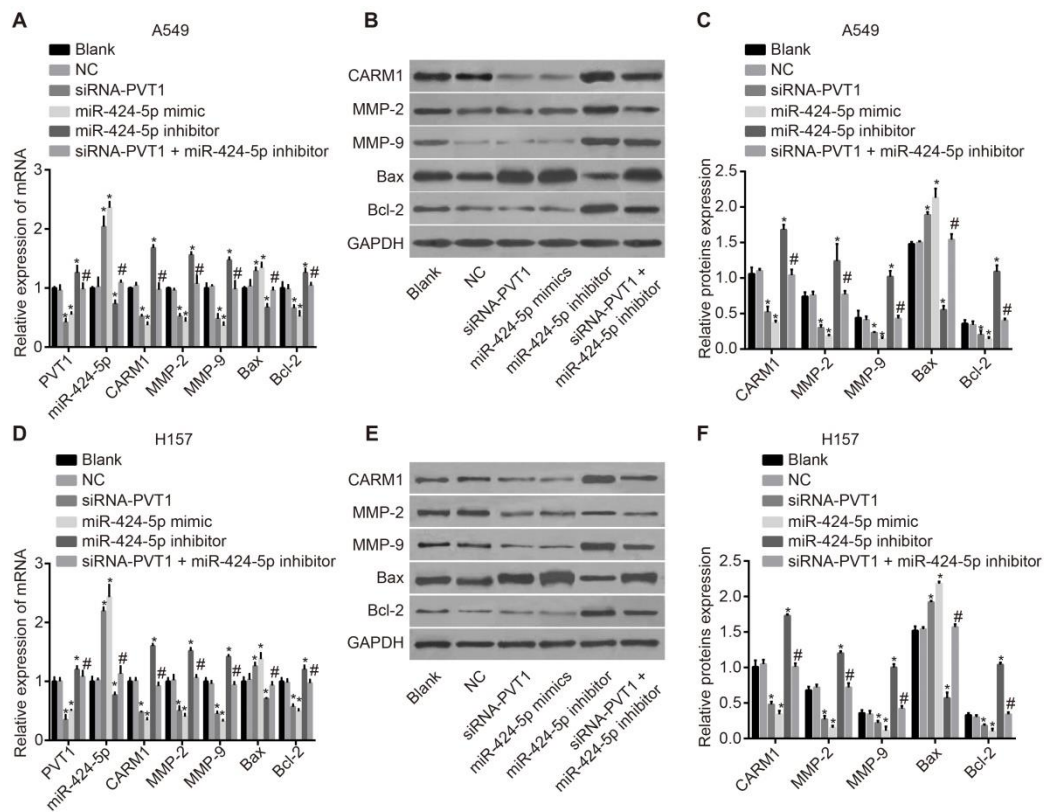
Supplementary Figure 4. The interaction of PVT1 and CARM1

Note: *, $P < 0.05$, compared with the IgG NC group. Data are means ± standard deviation from three independent experiments, P calculated by one way ANOVA; PVT1, plasmacytoma variant translocation 1; CARM1, co-activator associated arginine methyltransferase 1.
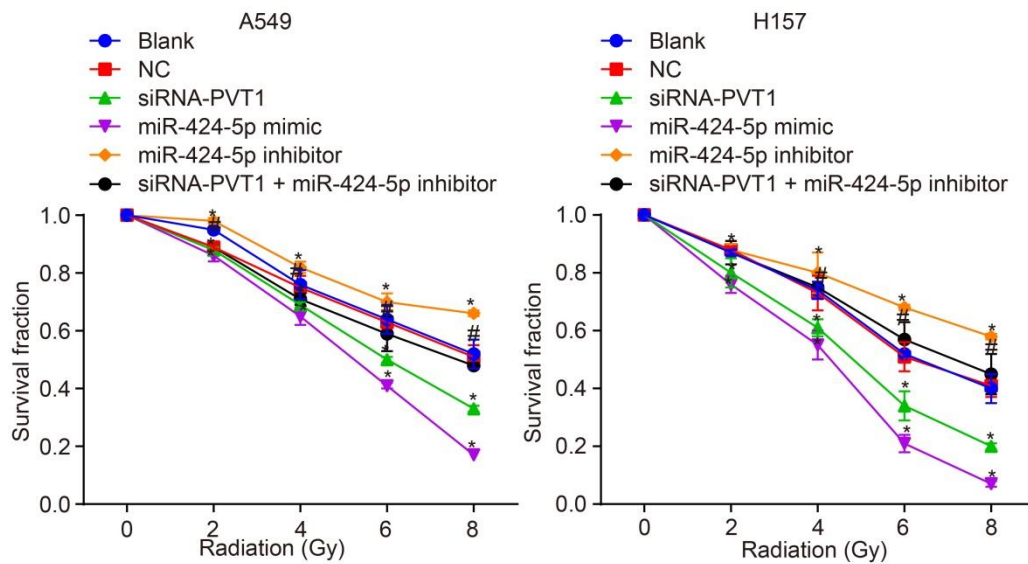
Supplementary Figure 5. Silencing of PVT1 or overexpression of miR-424-5p can increase the sensitivity of cell radiation to radiation

Note: [*], $P < 0.05$, compared with the blank and NC groups; [#], $P < 0.05$, compared with the siRNA-PVT1 group; Data are means ± standard deviation from three independent experiments, P calculated repeated measurement of analysis of variance; PVT1, plasmacytoma variant translocation 1; NC, negative control.
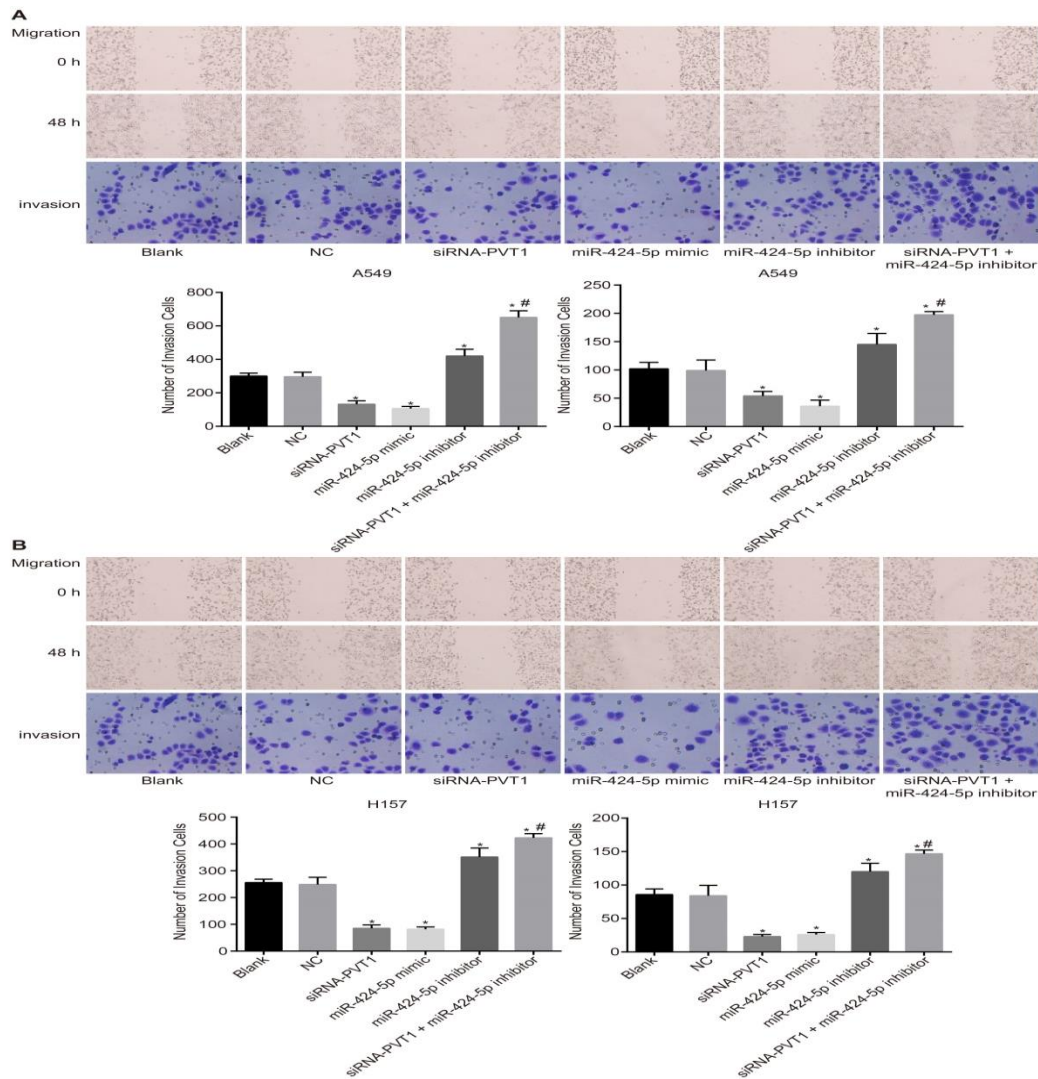
Supplementary Figure 6. siRNA-PVT1 or overexpressed miR-424-5p suppressed expression of CARM1 and some other factors related to tumor progression and cell apoptosis

Note: A & D, miR-424-5p expression and mRNA expression of PVT1, CARM1, MMP-2, MMP-9, Bcl-2 and Bax in cells; B & E, Western blot analysis; C & F, protein expression of PVT1, CARM1, MMP-2, MMP-9, Bax and Bcl-2 in cells; *, $P < 0.05$, compared with the blank and NC groups; #, $P < 0.05$, compared with the siRNA-PVT1 group; Data are means ± standard deviation from three independent experiments, P calculated by one way ANOVA; miR-424-5p, mircoRNA-424-5p; CARM1, co-activator associated arginine methyltransferase 1; MMP-2, matrix metallopeptidase-2; MMP-9, matrix metallopeptidase; Bcl-2, B cell lymphoma 2; Bax, Bcl2-associated X protein; PVT1, plasmacytoma variant translocation 1; NC, negative control.
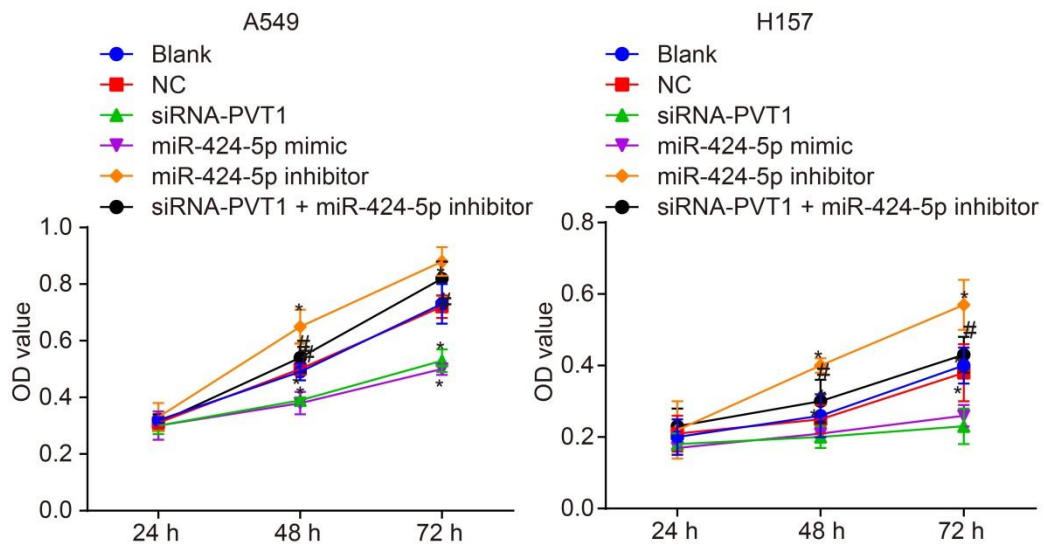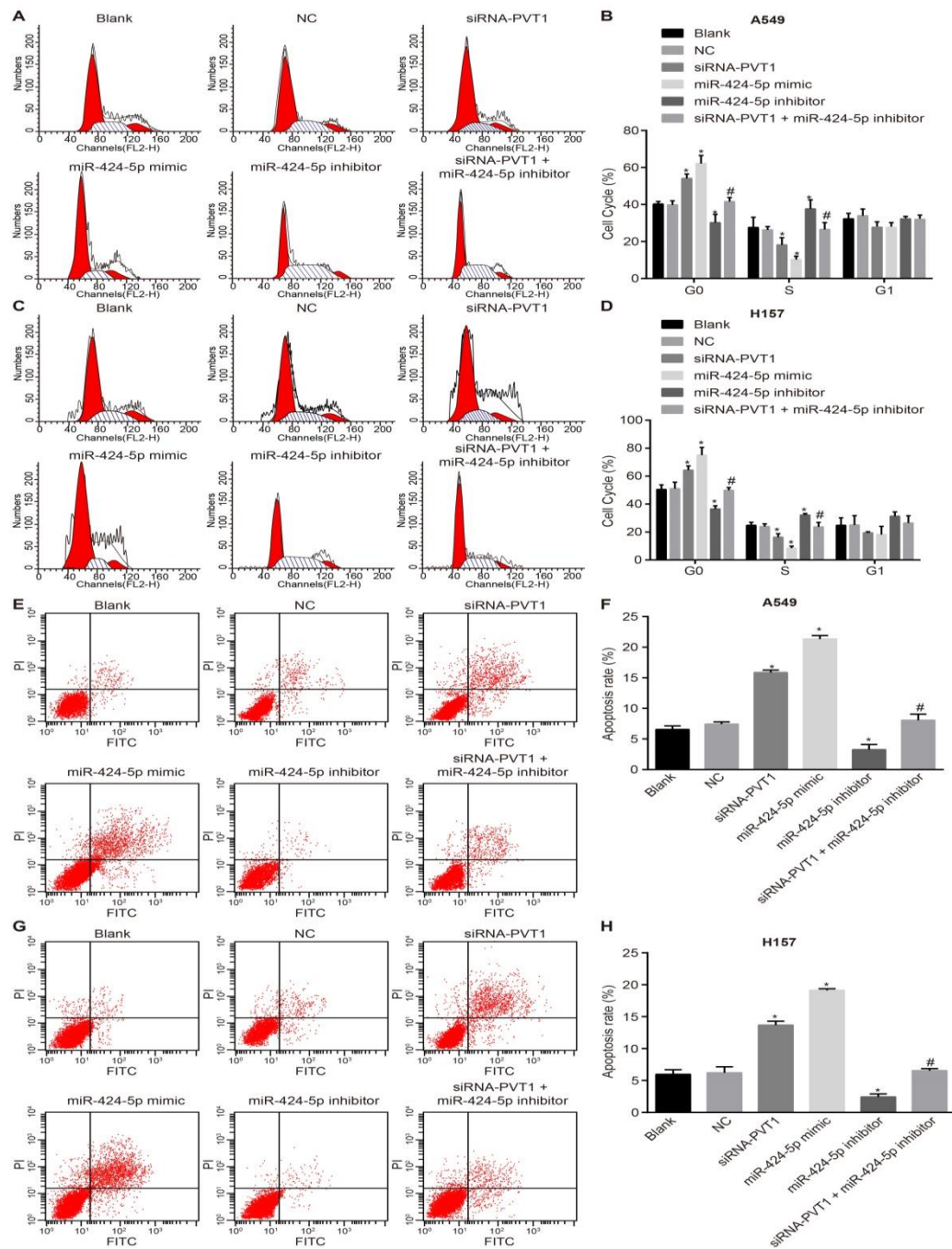
Supplementary Figure 7. NSCLC cell proliferation was inhibited after transfection of overexpressed miR-424-5p

Note: *, $P < 0.05$, compared with the blank and NC groups; #, $P < 0.05$, compared with the siRNA-PVT1 group; Data are means $\pm$ standard deviation from three independent experiments, P calculated repeated measurement of analysis of variance; PVT1, plasmacytoma variant translocation 1; miR-424-5p, mircoRNA-424-5p.

Supplementary Figure 8. NSCLC cell migration and invasion suppressed by siRNA-PVT1 or overexpressed miR-424-5p

Note: A, cell migration and invasion of A549 cell lines; B, cell migration and invasion of H157 cell lines; *, $P < 0.05$, compared with the blank and NC groups; $^\#$, $P < 0.05$, compared with the siRNA-PVT1 group; Data are means $\pm$ standard deviation from three independent experiments, P calculated by one way ANOVA; PVT1, plasmacytoma variant translocation 1; miR-424-5p, mircoRNA-424-5p.

Supplementary Figure 9. Changes of cell cycle distribution and apoptosis after transfection in each group

Note: A, cell cycle of A549 cell line; B, apoptosis of A549 cell line; C, cell cycle of H157 cell line; D, apoptosis of H157 cell line; *, $P < 0.05$, compared with the blank and NC groups; $^\#$, $P < 0.05$, compared with the siRNA-PVT1 group. Data are means $\pm$ standard deviation from three independent experiments, P (cell apoptosis) calculated by one way ANOVA; P (cell cycle) calculated repeated measurement of analysis of variance.
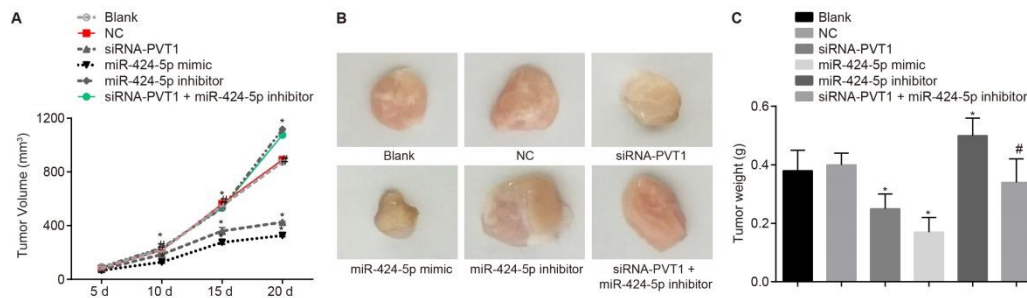
Supplementary Figure 10. Tumor growth was inhibited in A549 cell lines by siRNA-PVT1 or overexpressed miR-424-5p

Note: A, tumor growth graph; B, tumor size at the 20th day after radiation; C, tumor weight at the 20th day after radiation; *, $P < 0.05$, compared with the blank and NC groups; $^\#$, $P < 0.05$, compared with the siRNA-PVT1 group; Data are means ± standard deviation from three independent experiments, P (tumor weight) calculated by one way ANOVA; P (tumor volume) calculated repeated measurement of analysis of variance; n = 6 per group. PVT1, plasmacytoma variant translocation 1; miR-424-5p, mircoRNA-424-5p